Bažant, Z.P., and Pijaudier-Cabot, G. (1988). "Non- local continuum damage and measurement of characteristic length." in Mechanics of Composite Materials—1988, AMD 92, ed. by G. J. Dvorak and N. Laws, Am. Soc. of Mech. Engrs., N.Y. (Joint ASME/SES Conference, Berkeley, CA), 79–85.

AMD-Vol. 92

Mechanics of Composite Materials — 1988

presented at

THE JOINT ASME/SES APPLIED MECHANICS
AND ENGINEERING SCIENCES CONFERENCE
BERKELEY, CALIFORNIA
JUNE 20—22, 1988

sponsored by

THE COMMITTEE ON COMPOSITE MATERIALS OF
THE APPLIED MECHANICS DIVISION, ASME

edited by

G. J. DVORAK
INSTITUTE CENTER FOR COMPOSITE MATERIALS
AND STRUCTURES
RENSSELAER POLYTECHNIC INSTITUTE

N. LAWS
DEPARTMENT OF MECHANICAL ENGINEERING
UNIVERSITY OF PITTSBURGH

THE AMERICAN SOCIETY OF MECHANICAL ENGINEERS
United Engineering Center 345 East 47th Street New York, N.Y. 10017

NONLOCAL CONTINUUM DAMAGE AND MEASUREMENT OF CHARACTERISTIC LENGTH

Z. P. Bazant and G. Pijaudier-Cabot
Center for Concrete and Geomaterials
Northwestern University
Evanston, Illinois

ABSTRACT

Damage such as cracking or void formation is in many materials distributed and localizes only to a limited extent. The macroscopic treatment of such materials calls for a continuum description of damage, and this in turn necessitates a nonlocal definition of damage. Reasons for the nonlocal approach are briefly reviewed and the nonlocal damage model is summarized. Detailed attention is then focused on the experimental determination of the characteristic length which enters the spatial weighting function and characterizes the nonlocal properties of the material. The basic idea is to compare the response of two types of specimens, one in which the tensile softening damage remains distributed and one in which it localizes. The latter type of specimen is an edge-notched tensile fracture specimen, and the former type of specimen is of the same shape but without notches. Localization of softening damage is prevented by gluing to the specimen surface a layer of parallel thin steel rods and using a cross section of a minimum possible thickness that can be cast with a given aggregate. The characteristic length ℓ is the ratio of the fracture energy (i.e., the energy dissipated per unit area, dimension J/m^2) to the energy dissipated per unit volume (dimension J/m^3). Evaluation of these energies from the present tests yields $\ell = 2.7$ times the maximum aggregate size for concrete.

REVIEW OF NONLOCAL DAMAGE CONCEPT

Despite the existence of powerful finite element programs, realistic predictions of failure of structures cannot be accomplished for the case of brittle heterogeneous materials such as concrete, rocks, certain ceramics, ice, wood and various composites, which are characterized by distributed damage or cracking. The problem is the macroscopic strain-softening which causes localization instabilities, spurious mesh sensitivity and incorrect convergence. These difficulties may be overcome by developing a nonlocal damage model for such materials.

One very effective version of the nonlocal concept is the nonlocal continuum with local strain (1,6). The key idea is to prevent localization of damage to regions of zero volume by a nonlocal formulation of the stress-strain relation in which only the damage, i.e., strain-softening response is nonlocal while the elastic response is local. In contrast to the original nonlocal constitutive model in which all the variables were nonlocal, several modeling advantages are gained by this idea:

(1) Imbrication (overlapping) of finite elements, which was required in the original formulation and has complicated programming, becomes unnecessary due to

the aforementioned idea, i.e., the usual finite element meshes can be used. (2) In contrast to the original totally nonlocal model, the differential equations of equilibrium for stresses, along with the boundary conditions, have the usual, classical form, i.e., the previous use of differential equilibrium equations, boundary conditions and interface conditions with higher-order terms is avoided; this further means that the continuity requirements for finite elements remain the same as for the usual, local finite element codes. (3) The new formulation has been proven to exhibit no zero-energy spurious modes of instability, which were present in the original totally nonlocal formulation and had to be suppressed by various artificial measures.

It is rather simple to prove mathematically that, with the concept of nonlocal damage, the energy dissipation cannot localize into regions of vanishing volume. This has been verified by extensive numerical simulations in one as well as two-dimensions (3-6).

The nonlocal damage formulation can take various forms depending on the type of application. For predominantly tensile cracking, considered smeared, a simple prototype relation of strain tensor ε_{ij} to stress tensor σ_{km} is (8):

$$\varepsilon_{ij} = [C_{ijkm} + n_i n_j n_k n_m \frac{\bar{\omega}}{(1-\bar{\omega})E'}] \sigma_{km} \tag{1}$$

in which C_{ijkm} = elastic constants, n_i = maximum principal strain direction, E' = constant, and $\bar{\omega}$ = nonlocal damage, which is calculated as

$$\bar{\omega} = f(\bar{\varepsilon}_I), \qquad \bar{\varepsilon}_I(\underset{\sim}{x}) = \int_V \alpha'(\underset{\sim}{x},\underset{\sim}{s}) \langle \varepsilon_I(\underset{\sim}{s}) \rangle dV \tag{2}$$

in which $\langle\ \rangle$ = positive part, ε_I = maximum principal strain, $\bar{\varepsilon}_I$ = nonlocal maximum principal strain, $\underset{\sim}{x}$, $\underset{\sim}{s}$ = coordinate vectors, V = volume of the body, and α' = empirical weighting function defined by the characteristic length of the material.

When the material is characterized by unloading at roughly constant slope, the softening damage may alternatively be described by a plasticity model with a degrading yield limit; this approach has also been generalized to a nonlocal form (8), considering the yield limit as a function of the nonlocal inelastic strain.

A rather powerful approach is a nonlocal formulation of the microplane type in which the stress-strain relation is characterized separately on the planes of various orientations and the global response is obtained by summing the contributions from all these planes on the basis of energy equivalence (variational principle). In this formulation, the concept of nonlocal damage is applied on the individual microplanes.

It turns out that the nonlocal damage concept is relatively easy to implement in large codes. All that needs to be done is to determine at each integration point of each finite element in each loading step the nonlocal average of strain or some other quantity, and then, based on it, calculate the new value of the damage variable. Using a supercomputer, such calculations have already succeeded for problems with several thousand nodes, such as the problem of cave-in of a subway tunnel in a soil stabilized by cement grouting, which exhibits strain-softening damage (8).

CHARACTERISTIC LENGTH AND ITS METHOD OF MEASUREMENT

The characteristic length, ℓ, is needed to define the weighting function $\alpha'(\underset{\sim}{x},\underset{\sim}{s})$ used in spatial averaging integrals such as Eq. 2. A convenient definition is (6,2)

$$\alpha'(\underset{\sim}{x},\underset{\sim}{s}) = \frac{\alpha(\underset{\sim}{x}-\underset{\sim}{s})}{V_r(\underset{\sim}{x})}, \qquad V_r(\underset{\sim}{x}) = \int_{V(\underset{\sim}{x})} \alpha(\underset{\sim}{x}-\underset{\sim}{s}) dV(\underset{\sim}{s}) \tag{3}$$

with

$$\alpha(\underset{\sim}{x}-\underset{\sim}{s}) = e^{-(k(\underset{\sim}{x})/\ell)^2} \tag{4}$$

in which for one dimension, $|\underset{\sim}{x}| = x^2$, $k = \sqrt{\pi} = 1.772$; for two dimensions, $|\underset{\sim}{x}| = x^2 + y^2$, $k = 2$; and for three dimensions, $|\underset{\sim}{x}|^2 = x^2 + y^2 + z^2$, $k = (6/\sqrt{\pi})^{1/3} = 2.149$. $V_r(\underset{\sim}{x})$ is a normalizing coefficient which assures that the integral of $\alpha'(\underset{\sim}{x},\underset{\sim}{s})$ over the entire body is always 1 for any point $\underset{\sim}{x}$.

To determine the characteristic length, the basic idea is to measure the

response of two types of specimens which are as similar as possible but such that in one type of specimen the damage, such as cracking, remains nearly homogeneously distributed while in the other type it localizes to the minimum volume that is possible for the given material.

The restrained and unrestrained specimens shown in Fig. 1 were selected. As is seen from the enlarged cross section at the bottom of Fig. 1, the longer sides of the rectangular cross section are restrained by gluing to them with epoxy a system of regularly spaced thin steel rods, which have relatively large gaps between them. These gaps, filled partially by epoxy, are quite deformable, because the elastic modulus of epoxy is much lower than that of concrete. Consequently, the set of thin steel rods cannot develop any significant transverse stresses, and thus cannot interfere appreciably with the Poisson effect in concrete. Furthermore, by choosing the cross sections of the rods to be much smaller than the

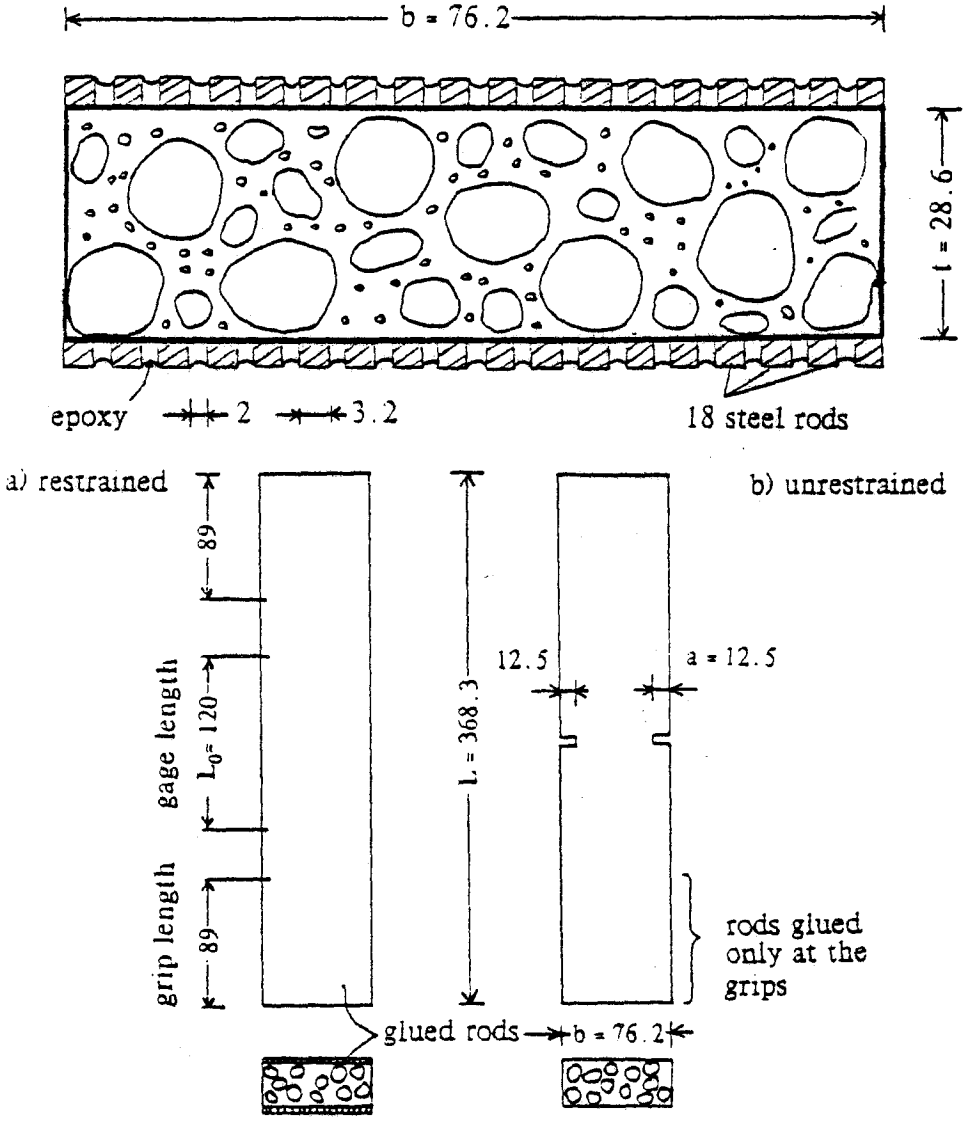

Fig. 1 Notched and unnotched specimens: cross section (top), side view (bottom)

maximum aggregate size, the thin rods cannot affect the nonlocal properties of the material in the transverse direction. The rectangular cross section is elongated, so as to minimize the influence of the wall effect and the local stresses near the short sides of the cross section.

The thickness of the cross section was chosen to be only 3-times the maximum aggregate size. The reason for this was to assure that the restraint due to steel rods affects the entire thickness of the specimen. For much thicker specimens, the restraint of the interior would be incomplete, and the strains could localize in the middle of the thickness.

The dimensions of the specimen are all indicated in Fig. 1. The ratio of water-cement-sand-gravel in the mix was 1:2:2:0.6, and the maximum size of the aggregate was d_a = 9.53mm. ASTM Type I cement was used. The specimens were removed from their plywood forms at 24 hours after casting and were then cured for 28 days in a room of relative humidity 95% and temperature 80°F.

The combined total cross section of the steel rods was selected so as to assure that the tangential stiffness of both the restrained and the unrestrained specimen would always remain positive. Consequently, the stability of the specimen and strain localization could not depend on the stiffness of the testing machine.

At the ends of the specimen, metallic grips were glued by epoxy to the surface of the steel rods. In the companion unrestrained specimens, the surface steel rods were glued to the grips only within the area under the grips. To assure the tensile crack to form away from the grips and run essentially normal to the axis, notches (of thickness 2.5 mm), were cut by a saw into the unrestrained specimens (Fig. 1).

The specimens were tested in tension in a closed-loop testing machine. The loading was stroke controlled and was made at a constant displacement rate which was 2×10^{-5}/s. Relative displacements on a base length of 120 mm (Fig. 1) were measured by two symmetrically placed LVDT gages mounted on one face of the specimen, attached to the steel rods. Three specimens of each type were tested but only two tests on unrestrained specimens could be exploited because of technical difficulties in setting up the experiment.

The plot of the average load versus displacement (mean of the measurements from the two LVDTs for each test) for the restrained and unrestrained specimens, which exhibit distributed and localized cracking, are shown in Fig. 2. The results confirm that the incremental stiffness has indeed always been positive. It is seen that for the unrestrained specimens (unbonded rods) the load displacement curve quickly approaches that for the steel rods alone. On the other hand, for the restrained specimens the response curve remains for a long time significantly higher than that for the steel rods alone.

No macrocracks were observed on the short exposed sides of the restrained specimens, but a series of tiny microcracks could be detected. It was also noticed that microcracking was somewhat more extensive farther away from the surface of the specimen, which is explained by the restraint of the steel bars.

The results for the restrained specimens from Fig. 2 were converted to stress-strain curves for the restrained specimens with distributed damage; see Fig. 3. The final portion of the softening curve (shown dashed) had to be estimated by analogy with other test data. It may be noted that the relative scatter of the results in Fig. 3 is increased by the fact that the force in the steel is subtracted from the measured force values. This may explain why the measured response curve is not very smooth.

EVALUATION OF CHARACTERISTIC LENGTH FROM TEST RESULTS

Taking the continuum viewpoint, we may consider the distributions of the macroscopic longitudinal normal strain along the gage length of the specimen to be uniform for the restrained specimen, and localized, with a piecewise constant distribution, for the unrestrained specimen. Further we assume that this localization begins to develop right at the peak stress point. The fact that localization begins right at the peak stress point is indicated by some recent measurements of deformation distributions in tensile specimens (Raiss (5)).

The energy, U_s, that is dissipated due to fracturing in the unbonded specimen with localized strain was determined as the area under the curves of axial force P versus axial relative displacement u for loading and for unloading from

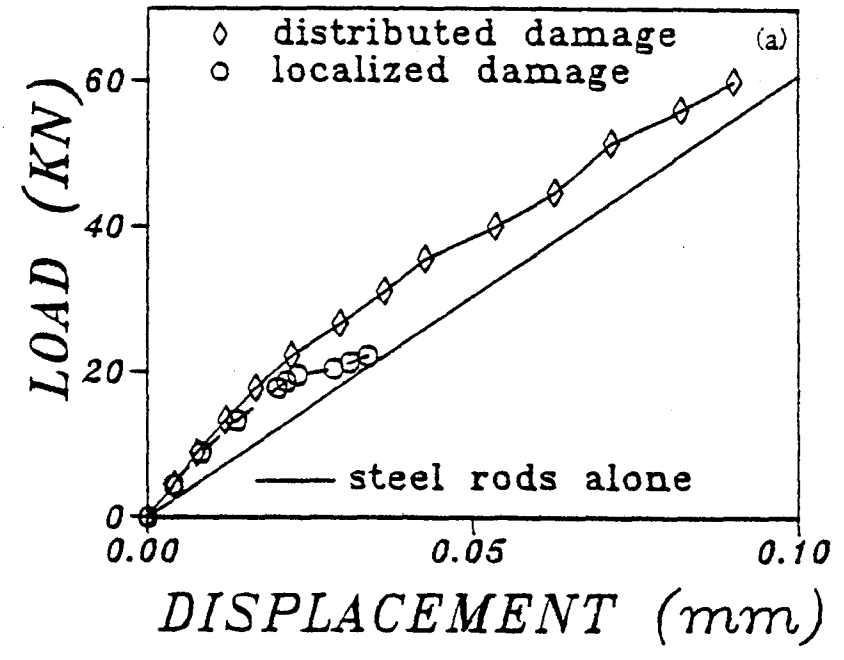

Fig. 2 Measured load-displacement curve of unnotched bonded specimen

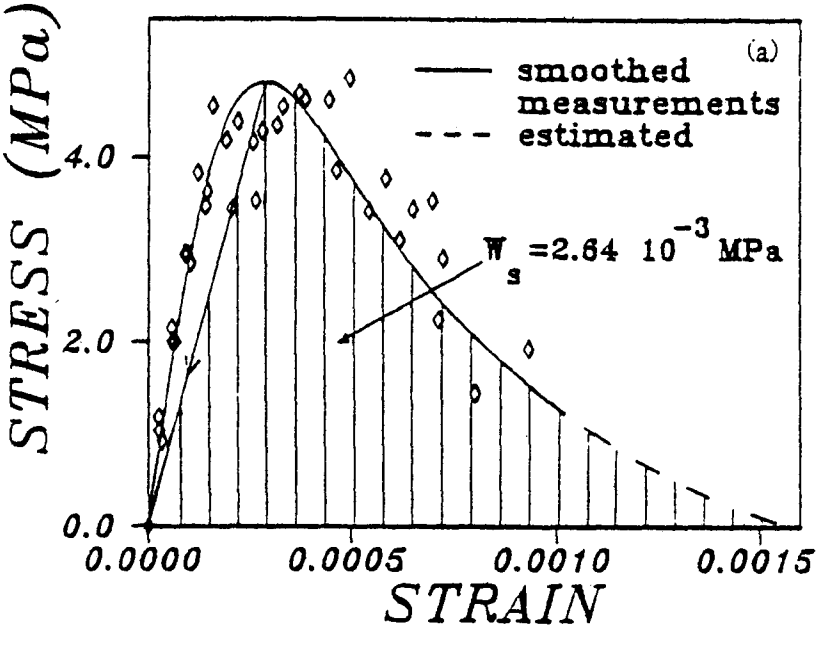

Fig. 3 Stress-strain curve obtained from unnotched bonded specimens

the peak stress point. We may now define the effective width h of the localized strain profile to be such that the stress-strain diagram for the localization zone (fracture process zone) would be the same as that for the bonded specimen with a homogeneous strain distribution. Thus, the balance of energy requires that $G_f = hW_s$ where $G_f = U_s/A_0$ = fracture energy of the material (dimension N/m), and A_0 is the cross section area of the net (ligament) cross section of the notched specimen. From this, the effective width of the localization zone is obtained as

$$h = \frac{G_f}{W_s} . \tag{5}$$

The characteristic length of the nonlocal continuum can now be determined; however, the precise formulation of the nonlocal continuum must be specified. We consider the nonlocal continuum formulation from Bažant and Pijaudier-Cabot (3) (1987b), in which nonlocal averaging is applied only to damage and all other variables are treated as local. For this nonlocal damage theory, the profile of the continuum strain within the localization zone of a tensile specimen has been calculated in Bažant and Pijaudier-Cabot (1987b). This nonlocal formulation is equivalent in terms of the overall displacement if the area under the curved strain profile is the same as the area under the rectangular strain profile which was implied in evaluating the test results according to Eq. 1. From the shape of this curve, one finds that the areas are equal if $h_1 = \alpha h$, in which $\alpha = 1.93$ and h_1 = width of the zone of localized damage. Furthermore, for this nonlocal continuum model it has been shown that $h_1 = \beta \ell$, in which $\beta = 1.89$. It follows that

$$\ell = \frac{\alpha G_f}{\beta W_s} . \tag{6}$$

Coefficients α and β are particular to the chosen type of nonlocal continuum formulation. For the one considered here they yield $\alpha/\beta = 1.02$. Thus, the characteristic length is essentially the same as the width of the strain-softening zone under the assumption of a uniform strain within the zone. This is approximately true also for other variants of the nonlocal continuum formulation, and so we have, approximately

$$\boxed{\ell \simeq \frac{G_f}{W_s} .} \tag{7}$$

G_f and W_s have been evaluated from the measurements. The result is

$$\ell = 2.7\ d_a \tag{8}$$

in which d_a is the maximum aggregate size.

The value of the characteristic length obtained in Eq. 7 for the present experiments is consistent with previous estimates obtained in calibrating the crack band model proposed by Bažant and Oh (Ref. 1). At that time the characteristic length was inferred indirectly, by using only the fracture test results and optimizing their fits for specimens of various geometries and sizes, made from different concretes. In that study, the optimum fit was obtained approximately for $\ell = 3d_a$.

In closing it should be noted that the present tests bear some similarity with the tests by which L'Hermite (4) discovered strain-softening of concrete. He tested with his co-workers specimens made by casting concrete into a steel pipe with an internal thread. Bonded to concrete by the thread, the steel pipe was loaded in tension and transmitted the tensile force to concrete. Since the pipe was elastic, the force it carried was easily determined by measuring the deformation of the pipe, and the remainder of the tensile force could be ascribed to concrete. The steel pipe no doubt prevented the tensile cracking from localizing into a single major crack. Companion tests in which concrete was bonded to the pipe only near the grips revealed significant differences in the strength limit and the post-peak behavior. L'Hermite's tests, however, had a drawback due to the fact that the steel envelope has a higher Poisson ratio than concrete. As a result, the concrete in the pipe must have been subjected in these tests to significant lateral compressive stresses producing a confinement effect. Therefore,

these tests cannot be regarded as uniaxial and the presence of triaxial stresses complicates interpretation of the measurements.

ACKNOWLEDGMENT

The experiments were supported by U.S. Air Force Office of Scientific Research under contract F49620-87-C0030DEF with Northwestern University, monitored by Dr. Spencer T. Wu, and the theoretical work was supported by U.S. National Science Foundation under Grant MSM-8700830, monitored by Dr. Albert S. Kobayashi.

REFERENCES

1. Bažant, Z. P., and Oh, B. H., "Crack Band Theory for Fracture of Concrete," Materials and Structures, RILEM, Paris, France, Vol. 16, 1983, pp. 155-177.

2. Bažant, Z. P., and Pijaudier-Cabot, G., "Modeling of Distributed Cracking by Nonlocal Continuum with Local Strain," Proc., 4th Intern. Conf. on Numerical Methods in Fracture Mechanics, held in San Antonio, Texas, ed. by A. B. Luxmoore et al., Pineridge Press, Swansea, U.K., 1987a, pp. 411-432.

3. Bažant, Z. P., and Pijaudier-Cabot, G., "Nonlocal Damage: Continuum Model and Localization Instability," Report No. 87-2/428n-I, Center of Concrete and Geomaterials, Northwestern University, Evanston, Illinois, 1987b; see also "Nonlocal Damage, Localization Instability and Convergence," Journal of Applied Mechanics, ASME, in press.

4. L'Hermite, R., "Volume Changes of Concrete," 4th Int. Symp. on the Chemistry of Cement, Washington, 1960, pp. 659-702.

5. Raiss, M. E., "Observation of the Development of Fracture Process Zone in Concrete under Tension," Ph.D. Thesis, 1986, Imperial College, London, U.K.

6. Pijaudier-Cabot, G., and Bažant, Z. P., "Nonlocal Damage Theory," J. of Engng. Mech. ASCE, Vol. 113, Oct. 1987, pp. 1512-1533.

7. Bažant, Z. P. , and Lin, F.-B., "Nonlocal Yield Limit Degradation," Intern. J. of Numerical Methods in Engineering, in press; see also Preprints, Int. Conf. on Computational Plasticity, held in Barcelona, Apr. 1987, ed. by E. Oñate, R. Hinton, E. Owen, Univ. of Wales, Swansea, 1987, pp. 1757-1779.

8. Bažant, Z. P., and Lin, F.-B., "Nonlocal Smeared Cracking Model for Concrete Fracture," J. of Engng. Mech. ASCE, in press; also Report No. 87-7/498ns, Center for Concrete and Geomaterials, Northwestern University, Dec. 1987.